Enhanced Near-Field Heat Flow of a Monolayer Dielectric Island

Ludwig Worbes, David Hellmann, and Achim Kittel*
Institut für Physik, Carl von Ossietzky Universität, D-26111 Oldenburg, Germany
(Received 27 November 2012; published 28 March 2013)

We have investigated the influence of thin films of a dielectric material on the near-field mediated heat transfer at the fundamental limit of single monolayer islands on a metallic substrate. We present spatially resolved measurements by near-field scanning thermal microscopy showing a distinct enhancement in heat transfer above NaCl islands compared to the bare Au(111) film. Experiments at this subnanometer scale call for a microscopic theory beyond the macroscopic fluctuational electrodynamics used to describe near-field heat transfer today. The method facilitates the possibility of developing designs of nanostructured surfaces with respect to specific requirements in heat transfer down to a single atomic layer.

DOI: 10.1103/PhysRevLett.110.134302 PACS numbers: 44.40.+a, 65.80.−g, 68.37.Ef, 68.37.Uv

The heat transfer mediated by electromagnetic fields consists of two channels: on the one hand via blackbody radiation described by the Stefan-Boltzmann law and on the other hand via evanescent modes. The contribution of the latter increases significantly when the distance between these bodies is smaller than the dominant thermal wavelength, which is about 10 μm at room temperature. This thermal proximity effect, which is due to the overlap of evanescent waves tied to the bodies' surfaces, has been studied theoretically for decades [1–3]. The accepted theoretical description of near-field heat transfer is based on fluctuational electrodynamics [4], relying on the macroscopic Maxwell equations together with linear-response theory in the form of the fluctuation-dissipation theorem [5,6].

But only recently has this important phenomenon received growing experimental attention [7–15]. The increase of heat flow with decreasing distance has been demonstrated under well-controlled conditions [7,13,14], and it has been shown that the near-field heat flow easily exceeds the far-field limit expressed by the Stefan-Boltzmann law [9,10]. In particular, the contribution of thermally excited surface polariton modes [8] can enhance the heat transfer by several orders of magnitude [16]. This finding, which can be attributed to an increased number of contributing modes or heat flow channels [17,18], explains why most measurements use materials like silica or sapphire which support such surface modes in the infrared, accessible to thermal excitation at moderate temperatures [9–12,14].

The different experiments can be distinguished in two categories. First, plate-plate or plate-sphere setups enable measurements at distances from the micrometer range down to some 10 nm with a high resolution of the heat flow [9–15]. These experiments measure the integrated heat flow over an area of a few square micrometers to square centimeters. The experimental data for bulk samples [12,14,15] are in very good agreement with the theoretical approach. Second, there are setups employing a microscopic scanning probe to measure the evanescent modes spatially resolved [7,8]. There are several theoretical works, based on the framework of fluctuational electrodynamics, which predict that thin material layers on a substrate can substantially enhance the heat flow [3,16–21]. This was the initial motivation of our studies described in the following.

In this Letter, we discuss spatially resolved measurements of near-field heat transfer beyond the previously accessible macroscopic regime: Using the near-field scanning thermal microscope (NSThM) developed and refined in our group [7,22] we demonstrate that a single ionic monolayer island of sodium chloride (NaCl) deposited on a gold surface [Au(111)] increases the heat flow between the microscope probe and the sample by a factor of 2 for sample-probe separations of a few nanometers. The results presented in this Letter call for a more refined theoretical approach.

The NSThM is a modified commercial ultrahigh-vacuum (UHV) variable-temperature scanning tunneling microscope (Omicron VT-STM). The STM probe has been functionalized to act also as a thermosensor [22]. A sketch of its working principle is shown in Fig. 1(a): the sample is cooled down to 135 K by a liquid-nitrogen flow cryostat, whereas the probe is held at room temperature. This applied temperature difference ΔT_0 between the probe and the sample drives a radiative heat flow $\dot{Q}$ across the vacuum gap. Since the thermal resistance of the probe is constant, any variation of the heat flow can be attributed to a variation of the thermal resistance of the vacuum gap. In particular, when the tip's apex dips into the thermal near-field of the sample, the evanescent modes yield an enhanced heat flow $\dot{Q}$ resulting in a detectable cooling of the tip's apex against the probe holder by $\Delta T_{\mathrm{probe}}$. Hence, a spatial-dependent heat flow $\dot{Q}$ results in a spatial-dependent temperature drop $\Delta T_{\mathrm{probe}}$. In order to measure the temperature drop $\Delta T_{\mathrm{probe}}$ the standard STM probe is replaced by a homemade probe featuring an integrated miniaturized thermocouple [22] which converts the

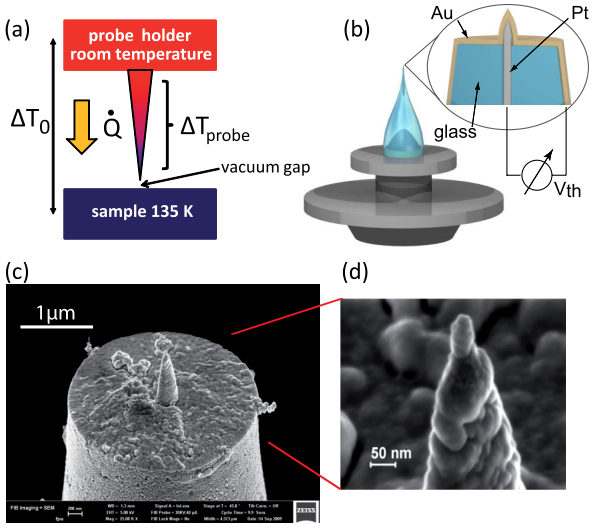

FIG. 1 (color online). (a) Schematics of the heat flow in the NSThM. The probe holder serves as a room-temperature heat bath for the probe while the sample is cooled down to 135 K. The overall temperature difference ΔT_0 causes a heat flow $\dot{Q}$ across the vacuum gap between the probe and sample. This heat flow is measurable as a slight temperature drop $\Delta T_{\mathrm{probe}}$ across the probe. (b) Schematic view of the probe in its Omicron-type tip holder; the right inset is the magnified cross section of the apex. At the contact point of Au and Pt a thermocouple is formed to measure $\Delta T_{\mathrm{probe}}$. The pointed apex serves as a tunneling probe. (c) scanning electron microscope (SEM) micrograph of the fore end of the actual sensor. (d) High-resolution SEM micrograph of the tunneling tip. Images were taken at Carl Zeiss, Oberkochen (Germany).

$\Delta T_{\mathrm{probe}}$ into a thermovoltage V_{th}, which is proportional to $\dot{Q}$ under the assumption that the Fourier law is valid and the Seebeck coefficient is constant.

A schematic view of such a NSThM probe is depicted in Fig. 1(b): the probe consists of a borosilicate glass pipette surrounding a 25 μm platinum core, processed by a micropipette puller. The platinum wire is protruding from the front end of the glass body by about 1 μm, forming a pointed tunneling probe with a tip apex radius in the range of 20–50 nm. It is evaporation coated with a nominally 20–200 nm thin film of gold. In this manner a thermocouple is realized in the contact region between the gold layer and the protruding platinum wire at the fore end of the glass body.

The decisive advantage of this setup lies in the fact that it can still be operated in the STM mode, which allows us to perform topographic measurements with atomic resolution of the sample while simultaneously recording the heat flow with the same positioning accuracy of the probe. Scanning electron micrographs of the foremost part of an actual NSThM probe are shown in Figs. 1(c) and 1(d); please note the apex radius, important for the STM functionality.

In the following NSThM experiments clean Au(111) surfaces were used as substrates for evaporated islands of NaCl. Our experiments are carried out in a UHV system with a base pressure below 2×10^{-10} mbar, while some preparation steps are performed in an attached high-vacuum preparation chamber with a base pressure below 2×10^{-7} mbar. Sample substrates of Au(111) films were prepared by evaporation of a 200 nm layer of gold onto cleaved mica by *e*-beam evaporation. The Au(111) samples were cleaned by cycles of sputtering (argon or oxygen, 2 kV, 2 μA, 10 min) and annealing (550 °C, 15 min, in UHV) after their transfer into the apparatus. NaCl was evaporated in the attached high-vaccuum chamber onto the substrates at room temperature by a home-built effusion cell at a temperature of 530 °C. The thickness of the NaCl films was determined by STM measurements. Probes are fully processed *ex situ*, but cleaned by hydrogen ion sputtering (650 V, 1 μA, 10 min) after being transferred into the vacuum system. The cleaning procedures were monitored by Auger electron spectroscopy.

Figure 2(a) shows a topographic STM image, obtained in the constant-current mode with a gold-platinum thermocouple probe, of a 500×500 nm^2-sized, atomically flat Au(111) surface. There are a few monoatomic steps

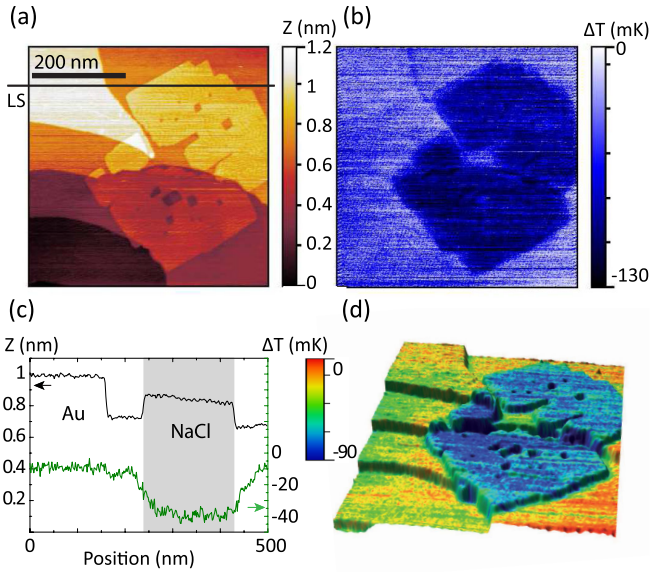

FIG. 2 (color online). (a) Topographic STM image of NaCl monolayer islands on an Au(111) surface with a few atomic steps (image size 500×500 nm^2, sample bias -600 mV, set point for the tunnel current 250 pA, sample temperature 145 K). (b) Temperature change ΔT of the tip's apex, acquired simultaneously with the STM image (image filtered at power line frequency 50/100 Hz). (c) Horizontal line scans of both topography (upper curve) and temperature change ΔT (lower curve), taken along the line labeled "LS" in (a). Please note that ΔT is almost unaffected by the gold step, but increases clearly above the NaCl layer. (d) A three-dimensional representation of the topographic data. The false color image of the temperature change is used to color the surface enabling a visual assignment of topographic structure and heat transfer.

partially covered by a single monolayer island of NaCl extending over the terraces of gold. The NaCl island exhibits several characteristic features like straight edges, 90° kinks, and a carpetlike overgrowth of the gold steps which are known from the literature.

Figure 2(b) depicts the spatially resolved temperature change of the probe's apex ΔT acquired simultaneously with the STM image. The relative temperature change ΔT is proportional to the change of near-field heat transfer between the probe and sample. One clearly observes an enhanced temperature drop corresponding to an increased thermal near-field coupling above the island. Figure 2(c) displays scans of both topography and temperature change ΔT along the line labeled "LS" in Fig. 2(a). Proceeding from left to right, the STM topographic signal sharply resolves the edge of the gold layer with a step height corresponding well to the expected height of about 240 pm for a monoatomic step on a Au(111) surface, followed by a NaCl island with an apparent height of about 140 pm, which is in agreement with other published measurements for NaCl monolayers on Au(111) [23] and other metals [24]. The Au step is hardly visible in the ΔT graph, but there is a temperature decrease of the probe of about 40 mK above the NaCl monolayer, signaling an increased near-field heat flow from the probe to the sample.

While the data displaying the temperature change in tunneling contact is sufficient to localize areas of different near-field coupling as visualized in Fig. 2(d), the quantitative change of heat flow is not accessible. A possibility to determine the quantitative change is to measure the sample-probe distance dependence of $\Delta T_{\mathrm{probe}}$ above both a noncovered gold surface, and above gold covered with a single NaCl monolayer. These measurements display the absolute temperature drop $\Delta T_{\mathrm{probe}}$ of the probe due to the influence of the near-field coupling at close distances. Results of such measurements are displayed in Fig. 3, which features a temperature drop of about 150 mK above gold, and of about 300 mK above NaCl. Based on the proportionality of the temperature drop $\Delta T_{\mathrm{probe}}$ to the heat flow $\dot{Q}$, one can directly assign an enhancement by a factor of 2 of the heat flow mediated by the near field to a monolayer of NaCl compared to a bare Au(111) surface.

We have also investigated the role of the probe's material by changing the probe's outer coating from gold to chromium. Figure 4 shows data concerning the topography and temperature change obtained with a chromium-platinum thermocouple probe: again, the enhanced heat flow above the NaCl island is clearly visible.

Controlling the position of the NSThM probe by using it as an STM probe suggests two possible problems while measuring near-field heat flow: the first is the material dependence of the sample-probe distance, and the second is the influence of the tunneling current on the measured heat flow.

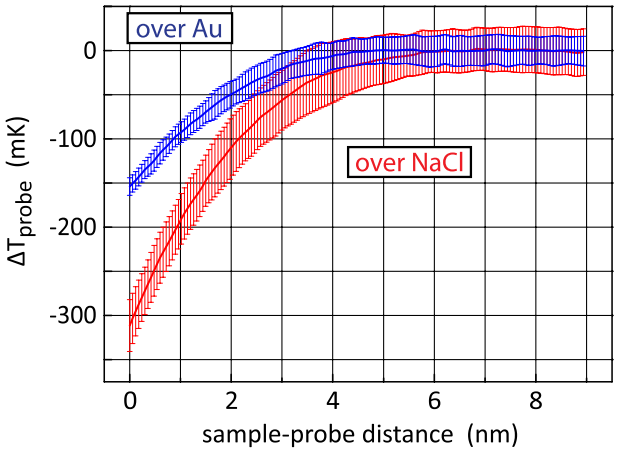

FIG. 3 (color online). $\Delta T_{\mathrm{probe}}$ measured versus the probe's distance to a noncovered Au(111) surface, and to a gold surface covered by a NaCl monolayer. With $\Delta T_{\mathrm{probe}} \propto \dot{Q}$, the heat flow $\dot{Q}$ is enhanced by a factor of 2 by a monolayer of NaCl compared to a Au(111) surface. For both measurements, the point of zero distance is defined by a tunneling current set point of 250 pA at a sample bias of -600 mV. Each curve is averaged over 10 measurements taken in the area depicted in Fig. 2; see the Supplemental Material [26] for the raw data.

In Fig. 2(a) the measured height of a NaCl island is about 140 pm. This value does not correspond to the geometrical height of a monolayer of NaCl, which amounts to 250–280 pm depending on the citation [23,24]. The difference of 110–140 pm is explained by the fact that the tunneling current at a fixed bias voltage depends on the work function and on the electronic density of states of the surfaces. When scanning in constant-current mode, the modified work function and/or electronic density of states above the NaCl layer forces the probe closer to the surface compared to the distance above noncovered areas of the gold surface. The pertinent question is whether the

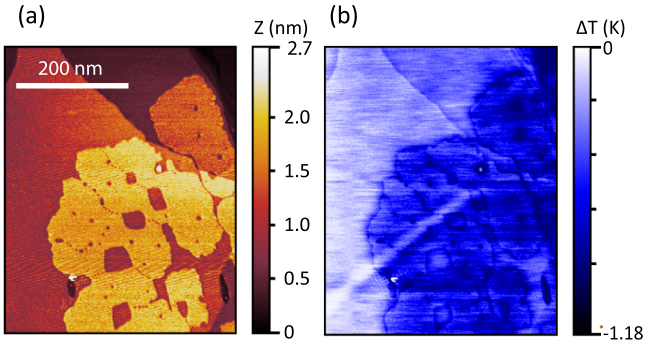

FIG. 4 (color online). (a) Topographic image of an Au(111) surface with several atomic steps, partially covered by a NaCl monolayer, as recorded with a chromium-platinum thermocouple probe (image size 400×500 nm^2, sample bias 600 mV, set point for the tunneling current 250 pA, sample temperature 135 K). (b) Temperature change image (image filtered at power line frequency).

increased near-field coupling observed in Fig. 2 can simply be explained by the reduction of the sample-probe distance. However, this possibility can be ruled out by the distance dependence of the temperature drop ΔT_{probe} displayed in Fig. 3. If the material dependence seen in Fig. 2(b) was entirely caused by the reduction of the sample-probe distance above the NaCl island by 110–140 pm, then it must be possible to bring the two curves in Fig. 3 into coincidence by shifting one of them horizontally with respect to the other by the same distance. Obviously, this is impossible: matching the two curves requires a shift of one by at least 1 nm, which is much more than the actual reduction of the sample-probe distance. Thus, Fig. 2(b) is no artifact caused solely by the variation of the work function and the local electronic density of states.

A second interpretation of Fig. 2(b) as an artifact, is to attribute the measured signal to crosstalk of the tunneling current on the measured thermovoltage. This seems possible in our setup because one leg of the thermocouple also acts as tunneling current drain. In order to exclude this we have measured the spatially resolved heat transfer at larger distances without a tunneling current being present. To this end, we have programmed our microscope controller such that after each line scan is recorded in the constant tunneling current mode, the trajectory of the probe is replayed with a specified distance offset, as sketched in Fig. 5(c). The topography of the sample surface employed for this check is shown in Fig. 5(a); it is only slightly displaced against that seen in Fig. 2(a). Figure 5(b) depicts the corresponding temperature change of the tip's apex in tunneling contact, whereas Fig. 5(d) displays the temperature change data obtained with an offset of 1 nm on the tunneling distance. The NaCl island is clearly discernible in both images, with a slightly decreased contrast for the larger recording distance. As seen in Fig. 5(e) there is no tunneling current at that large distance, but only interferences at power-line frequency with an amplitude below 25 pA. These results show that the thermovoltage signal represents the heat flow and confirm that thermal near-field coupling in our setup is of longer range than the electron tunneling distance.

The theoretical description by means of fluctuational electrodynamics was able to cover many observed phenomena of near-field heat transfer in the past incorporating processes caused by surface-plasmon-polaritons as for Au and surface-phonon-polaritons as for SiC or NaCl, but is inappropriate for the experimental situation here, because it is violating the conditions required for invoking macroscopic fields [25]. In the model of fluctuational electrodynamics, materials are treated by their macroscopic dielectric properties by means of complex and spatial homogeneous permittivity and permeability, which are determined by measurements on bulky samples. The NaCl islands are only a single atomic layer thick on a gold

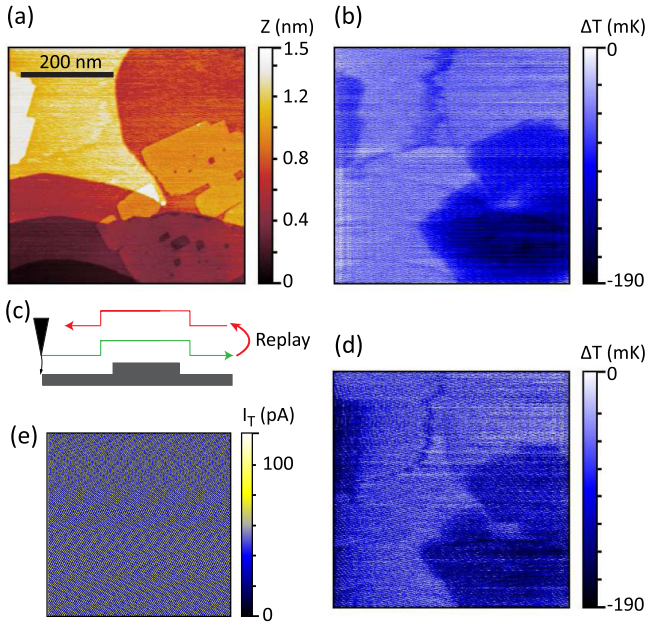

FIG. 5 (color online). (a) STM topographic image of a partially NaCl-covered gold surface, as in Fig. 2(a). (b) Temperature change of the tip's apex, recorded simultaneously with the topographic data while being in tunneling contact with the sample. (c) Procedure employed for scanning at distances larger than the tunneling distance: after scanning a line of the sample in constant-current mode, the scanning trajectory is replayed with a specified distance offset. (d) Temperature change of the tip's apex recorded with a distance offset of 1 nm [image (b) and (d) filtered at power line frequency]. (e) The tunneling current at that distance, recorded simultaneously with (d) is zero; only interference patterns at power-line frequency are visible (unfiltered data).

substrate. It is doubtful to assume bulk properties for such a layered system. Furthermore, fluctuations are assumed to be white; i.e. there is neither a limiting time scale nor a length scale. We have shown in an earlier work [7] that this is not correct. The fundamental assumptions are definitely violated; they seem to require a genuinely "atomic" theoretical approach. One possible additional pathway increasing the heat transfer could be a van der Waals–like coupling between the NaCl and the tip separated only from about a fraction of an atom's diameter to a few tens of atom's diameters leading to a force interaction. Thus phononic excitations of the NaCl ions will couple to the tip involving optical and acoustic phonons. These effects have to be covered or at least have to be proven to be negligible by a correct theoretical treatment.

To conclude, we have observed a definite enhancement, by a factor of about 2, of heat transfer at nanometer distances between the tip's apex of a NSThM probe and an Au(111) surface when the latter is covered by a single monolayer of NaCl. It will also be interesting to explore whether the near-field heat contrast caused by atomic layers can be exploited for novel forms of surface analysis.

Insights gained by the NSThM can assist finding the optimal design with respect to thermal management of nanometer-sized devices only a single atomic layer thick.

We thank Svend-Age Biehs and Martin Holthaus for fruitful discussions, Holger Koch for technical support, and Jürgen Parisi for constant support. This work was supported by the Deutsche Forschungsgemeinschaft (DFG), Project No. KI 438/8-1, and the EWE AG Oldenburg, Germany (EWE-Nachwuchsgruppe).

*kittel@uni-oldenburg.de

[1] D. Polder and M. Van Hove, Phys. Rev. B **4**, 3303 (1971).
[2] J. J. Loomis and H. J. Maris, Phys. Rev. B **50**, 18517 (1994).
[3] J. B. Pendry, J. Phys. Condens. Matter **11**, 6621 (1999).
[4] S. M. Rytov, Y. A. Kravtsov, and V. I. Tatarskii, *Principles of Statistical Radiophyics* (Springer, New York, 1989), Vol. 3.
[5] G. S. Agarwal, Phys. Rev. A **11**, 230 (1975).
[6] W. Eckhardt, Phys. Rev. A **29**, 1991 (1984).
[7] A. Kittel, W. Müller-Hirsch, J. Parisi, S.-A. Biehs, D. Reddig, and M. Holthaus, Phys. Rev. Lett. **95**, 224301 (2005).
[8] Y. De Wilde, F. Formanek, R. Carminati, B. Gralak, P.-A. Lemoine, K. Joulain, J. P. Mulet, Y. Chen, and J. J. Greffet, Nature (London) **444**, 740 (2006).
[9] L. Hu, A. Narayanaswamy, X. Chen, and G. Chen, Appl. Phys. Lett. **92**, 133106 (2008).
[10] A. Narayanaswamy, S. Shen, and G. Chen, Phys. Rev. B **78**, 115303 (2008).
[11] S. Shen, A. Narayanaswamy, and G. Chen, Nano Lett. **9**, 2909 (2009).
[12] E. Rousseau, A. Siria, G. Jourdan, S. Volz, F. Comin, J. Chevrier, and J.-J. Greffet, Nat. Photonics **3**, 514 (2009).
[13] T. Kralik, P. Hanzelka, V. Musilova, A. Srnka, and M. Zobac, Rev. Sci. Instrum. **82**, 055106 (2011).
[14] R. S. Ottens, V. Quetschke, S. Wise, A. A. Alemi, R. Lundock, G. Mueller, D. H. Reitze, D. B. Tanner, and B. F. Whiting, Phys. Rev. Lett. **107**, 014301 (2011).
[15] P. J. van Zwol, L. Ranno, and J. Chevrier, Phys. Rev. Lett. **108**, 234301 (2012).
[16] J.-P. Mulet, K. Joulain, R. Carminati, and J.-J. Greffet, Appl. Phys. Lett. **78**, 2931 (2001).
[17] P. Ben-Abdallah and K. Joulain, Phys. Rev. B **82**, 121419(R) (2010).
[18] S.-A. Biehs, E. Rousseau, and J.-J. Greffet, Phys. Rev. Lett. **105**, 234301 (2010).
[19] A. I. Volokitin and B. N. J. Persson, Phys. Rev. B **69**, 045417 (2004).
[20] S.-A. Biehs, Eur. Phys. J. B **58**, 423 (2007).
[21] M. Francoeur, P. Mengüç, and R. Vaillon, Appl. Phys. Lett. **93**, 043109 (2008).
[22] U. F. Wischnath, J. Welker, M. Munzel, and A. Kittel, Rev. Sci. Instrum. **79**, 073708 (2008).
[23] X. Sun, M. P. Felicissimo, P. Rudolf, and F. Silly, Nanotechnology **19**, 495307 (2008).
[24] F. E. Olsson, M. Persson, J. Repp, and G. Meyer, Phys. Rev. B **71**, 075419 (2005).
[25] J. D. Jackson, *Classical Electrodynamics* (New York, Wiley, 1998).
[26] See Supplemental Material at http://link.aps.org/supplemental/10.1103/PhysRevLett.110.134302 for the raw experimental data used to prepare Fig. 3.